Accepted Manuscript

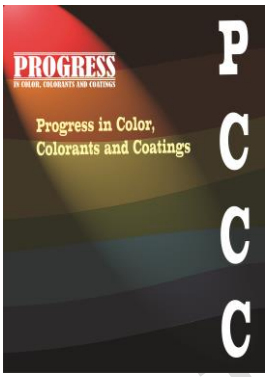

Title: Effect of Temperature and Cathodic Disbondment on the Performance of FBE and Hybrid Epoxy Coatings in Sabkha Soil and Persian Gulf Environments

Authors: Reza Amini, Pooneh Kardar

Manuscript number**: PCCC-2512-1479**

To appear in: Progresss in Color, Colorants and Coatings

Received: 14 December 2025

Final Revised: 4 March 2026

Accepted: 9 March 2026

Please cite this article as:

R. Amini, P. Kardar, Effect of Temperature and Cathodic Disbondment on the Performance of FBE and Hybrid Epoxy Coatings in Sabkha Soil and Persian Gulf Environments, Prog. Color, Colorants, Coat., 20 (2027) XX-XXX.

DOI: 10.30509/pccc.2026.167738.1479

Effect of Temperature and Cathodic Disbondment on the Performance of FBE and Hybrid Epoxy Coatings in Sabkha Soil and Persian Gulf Environments

R. Amini*, P. Kardar**

Department of Surface Coatings and Corrosion, Institute for Color Science and Technology, P.O. Box: 654-167665, Tehran, Iran.

Email: * amini-re@icrc.ac.ir; ** kardar@icrc.ac.ir

Abstract

Fusion-bonded epoxy (FBE) and a commercial hybrid epoxy were evaluated for their barrier performance and damage tolerance in simulated Sabkha soil and Persian Gulf seawater environments at 23 and 36 °C. The study utilized electrochemical impedance spectroscopy (EIS), linear polarization resistance (LPR), and adhesion testing to quantify coating degradation in intact, scratched, and cathodic disbondment (CD) scenarios. Results indicated a distinct performance trade-off: intact FBE exhibited superior primary barrier properties, maintaining a higher low-frequency impedance modulus ($>10^{10}$ Ω cm²) and lower capacitance than the hybrid system, which is attributed to its tighter microstructure. However, under damaged conditions coupled with cathodic protection, the hybrid epoxy demonstrated superior defect tolerance. While the FBE coating showed increased susceptibility to oxide lift and alkaline-induced delamination, particularly in Persian Gulf seawater at 36 °C, the hybrid system effectively resisted interfacial degradation, maintaining a NACE rating of 2 in the same aggressive environment. Mechanical testing confirmed that both systems possessed excellent initial adhesion with pull-off strengths consistently exceeding 1000 psi and cohesive failure modes. The

findings suggest that while FBE offers better initial isolation, the hybrid epoxy provides enhanced reliability in scenarios where mechanical damage and subsequent cathodic disbondment are the primary failure risks.

Keywords: Fusion-bonded epoxy; Hybrid Epoxy; Cathodic disbondment; Electrochemical impedance spectroscopy; Sabkha soil; Persian Gulf seawater.

1. Introduction

Generally speaking, pipelines provide the safest and most efficient way to transport oil and gas. Given the worldwide demand to ensure a stable energy supply, nothing is more important than preserving the integrity of these vital arteries [1, 2]. Buried pipelines, however, are continuously exposed to environmental risks, where leakage arising from damage may cause disastrous ecological damage. Corrosion is the process by which a material undergoes electrochemical interaction with its surrounding environment and is considered the principal cause of most pipeline failures [3, 4]. Recent estimates indicate that corrosion costs for U.S. energy extraction and petroleum-sector companies account for over half of total annual maintenance expenditures, totaling $170 billion. Fortunately, about a third of these costs could be avoided by applying appropriate materials and protection techniques [5-7].

In soil environments, several factors affect the corrosion of buried pipelines, including moisture content, temperature, pH, microbial activity, and, most importantly, dissolved salt concentration [8, 9]. The most problematic soil type for pipeline corrosion in the Persian Gulf region is "Sabkha" soil. Sabkha soil is highly saline, with a shallow

groundwater table and high levels of chloride and sulfate ions, making it extremely aggressive toward steel. Various studies have found that the presence of both sulfates and chlorides in synergy drastically accelerates corrosion rate, especially at high temperatures [10-13].

To mitigate these challenges, the common practice in the energy extraction and petroleum sectors is to adopt a multifaceted strategy that uses protective coatings as the first line of defence, supplemented by cathodic protection (CP). Coatings act by providing a physical barrier and high electrical resistance, thereby preventing the ingress of electrolyte onto the metal surface. Among the many coating types, fusion-bonded epoxy (FBE) is among the most widely used due to its excellent adhesion and high mechanical strength. However, FBE coatings can be vulnerable to water permeability and cathodic disbondment at elevated temperatures or when surface contamination is present. Hybrid epoxy coatings have been developed more recently to provide enhanced adhesion properties and lower curing temperatures. Nevertheless, there is scant information regarding their performance under cathodic protection at extreme conditions [14-18].

A serious problem arises when coatings develop defects or become detached from the metal surface, a process known as cathodic disbondment (CD). Under such conditions, when the cathodic protection current does not reach the disbonded area, the environment entrapped beneath the coating may increase the corrosion rate noticeably [19,20]. Increased temperature further accelerates coating degradation and deteriorates adhesion. Many of these processes can be investigated using sophisticated electrochemical techniques, such as electrochemical impedance spectroscopy (EIS), which can monitor changes in coating properties and at the metal/coating interface well before macroscopic

failure [21, 22].

Several studies have examined cathodic delamination and disbondment of epoxy-based coatings, often in NaCl media and/or using modified epoxy formulations, including hybrid/nanohybrid-filled epoxy systems designed to reduce delamination. Related work also reports the influence of cathodic polarization potential and temperature on the disbondment behavior of epoxy coatings. However, these studies generally do not provide a direct, head-to-head evaluation of commercial pipeline-grade FBE versus commercial hybrid epoxy under region-specific Sabkha soil brine and Persian Gulf seawater conditions within the 23-36 °C temperature range, particularly across intact, scratched, and cathodic-disbonded states [23-26]. Despite the extensive use of both FBE and hybrid epoxy coatings in pipeline applications, important knowledge gaps remain regarding their comparative performance under aggressive, region-specific service conditions. In particular, a systematic comparison under environments representative of Sabkha soil brine and Persian Gulf seawater, together with a temperature-dependent assessment, has been limited in the open literature. Moreover, many prior studies emphasize intact-barrier behavior, while fewer investigations compare coatings across realistic damage states (intact, mechanically damaged, and cathodic disbondment), where the governing failure mechanisms can change, and a trade-off between primary barrier performance and damage tolerance may emerge.

In this study, the corrosion-protection performance of a fusion-bonded epoxy (FBE) and a commercial hybrid epoxy coating applied to pipeline steel was evaluated under simulated service conditions in Sabkha soil brine and Persian Gulf seawater at 23°C and 36 °C. Coating effectiveness was assessed using electrochemical impedance spectroscopy

(EIS) and linear polarization resistance (LPR) to quantify barrier degradation and corrosion kinetics in intact and damaged conditions. Mechanical integrity and damage tolerance were further examined using pull-off adhesion testing (ASTM D4541) and cathodic disbondment (CD) testing coupled with knife tests (NACE RP0394). This combined approach aims to clarify temperature and environment-dependent degradation mechanisms and to provide guidance on selecting pipeline coatings for high-salinity environments.

2. Experimental

2.1. Materials and sample preparation

FBE and hybrid epoxy coatings were applied to carbon steel substrates measuring 150 × 50 mm and 5 mm thick. Surface preparation was performed by abrasive blasting in accordance with industrial standards to remove rust, mill scale, and contaminants, and to generate an anchor profile adequate for coating adhesion. The surface roughness profile prior to coating application was in the range of 51-102 µm for the FBE system and 64–114 µm for the hybrid epoxy system.

The hybrid epoxy coating used in this study consisted of a thermosetting epoxy resin matrix modified with additional polymeric and inorganic components to enhance adhesion, flexibility, and resistance to cathodic disbondment. The formulation included an epoxy base resin, a proprietary curing agent, and reinforcing fillers dispersed within the polymer matrix. The hybrid structure was designed to improve coating toughness and interfacial stability compared to conventional fusion-bonded epoxy while maintaining adequate barrier properties against electrolyte penetration. Both coatings were applied to

the carbon steel substrates according to the manufacturers' specifications to ensure uniform film formation and consistent curing behavior.

After coating application, the dry film thickness was measured to be 330-533 µm for the FBE specimens and 635-889 µm for the hybrid epoxy specimens. Although the coating thicknesses were not identical, each coating system was evaluated within its recommended industrial thickness range, ensuring a fair and application-relevant comparative assessment. For each coating system, the dry film thickness was measured at multiple locations and maintained within a consistent application range, and all reported electrochemical and mechanical data represent averaged values obtained from replicate specimens.

To assess coating performance under damaged conditions, several controlled defects, including standard scratches, holidays, and artificial cuts, were introduced on the coated surfaces. Controlled scratches were introduced on the coated specimens using a standardized scribing procedure to ensure repeatable defect geometry across all samples. The scratches were produced with uniform length and width sufficient to fully expose the steel substrate, and identical procedures were applied to all specimens. The consistency of the scratch dimensions was verified prior to testing to minimize variability in the electrochemical measurements associated with defect size.

Samples intended for microscopic examination were sectioned and subsequently wet-ground using silicon carbide papers with grit sizes of 300, 400, and 600. Final polishing was carried out using alumina suspensions of 0.5 and 1 µm, after which samples were rinsed with deionized water and air-dried to obtain high-quality surfaces suitable for microstructural characterization.

2.2. Test environments

Corrosion tests were performed in two synthetic aqueous media, specifically prepared to simulate the aggressive operational conditions of the Persian Gulf. Accordingly, the test media included a synthetic Sabkha solution, representative of highly saline soil brine, and a synthetic Persian Gulf seawater. The electrolyte solutions were prepared according to the required stoichiometry and the methods described by Kester, with modifications to match the local salinity characteristics [27].

In every test cycle, 75 mL of standardized electrolyte volume was maintained. Experiments were conducted at ambient and elevated temperatures (36 °C) to assess coating behavior under normal and accelerated conditions. Specimens were fully immersed in the corrosive media, and the solutions were refreshed periodically to maintain a stable ionic composition throughout the exposure period.

All electrochemical measurements were conducted under naturally aerated conditions, without intentional control or removal of dissolved oxygen, to replicate realistic service environments for buried pipelines in Sabkha soil and Persian Gulf seawater.

2.3. Techniques

Electrochemical testing, including OCP, LPR, Tafel polarization, and EIS, was conducted using a Gamry G750 system configured in a standard three-electrode configuration and was performed according to established methodologies. LPR measurements were made over a small potential range centered on E_{corr} using an automatic potential correction at a scan rate of 0.5 mV s^{-1}. Microstructural analyses were made using a JEOL JSM-6330F FE SEM operating under low-vacuum conditions and fitted with EDS for the purpose of

evaluating electrolyte penetration, damage morphology, and corrosion product formation. Tafel polarization measurements were used to corroborate corrosion current density trends obtained from LPR analysis and were therefore not discussed independently, as they did not introduce additional mechanistic information beyond the LPR and EIS results.

For SEM observation, coated specimens were sectioned from the test panels and prepared following standard metallographic procedures. The samples were sequentially wet-ground using silicon carbide papers with grit sizes of 300, 400, and 600 to expose the coating cross-sections and damaged regions. Final polishing was performed using alumina suspensions of 1 μm and 0.5 μm particle sizes to achieve a smooth, scratch-free surface suitable for microscopic examination. After polishing, the specimens were thoroughly rinsed with deionized water, ultrasonically cleaned in ethanol, and air-dried prior to SEM analysis. SEM imaging was performed to evaluate coating morphology, defect evolution, electrolyte penetration, and corrosion product formation at the coating/metal interface.

In addition, pull-off adhesion testing was conducted in accordance with ASTM D4541, and the modes of failure were categorized as adhesive, cohesive, or mixed. CD testing was conducted in accordance with ASTM G8 and ASTM G42 to assess coating resistance to delamination caused by cathodic polarization.

3. Results and Discussion

3.1. Barrier performance of intact coatings

The protective performance and initial barrier capability of intact FBE and Hybrid Epoxy

coatings were evaluated in simulated Sabkha soil and Persian Gulf water environments at 23 °C and 36 °C, using EIS. Impedance data were fitted using the EEC shown in Figure 1. In this equivalent electrical circuit, R_s represents the solution resistance of the electrolyte. The pore resistance of the coating is denoted by R_{po}, reflecting the resistance to ionic transport through coating defects and pores. The coating capacitance, C_c, corresponds to the dielectric behavior of the polymeric coating layer. In the equivalent electrical circuit, the constant phase elements (CPEs) were used instead of ideal capacitors to account for non-ideal electrochemical behavior. The exponent nC represents the deviation from ideal capacitive behavior of the coating layer and is associated with coating heterogeneity, dielectric dispersion, and water uptake. The exponent nM corresponds to the non-ideal capacitive response at the metal/coating interface and reflects surface roughness, interfacial inhomogeneity, and distributed charge-transfer processes [28, 29].

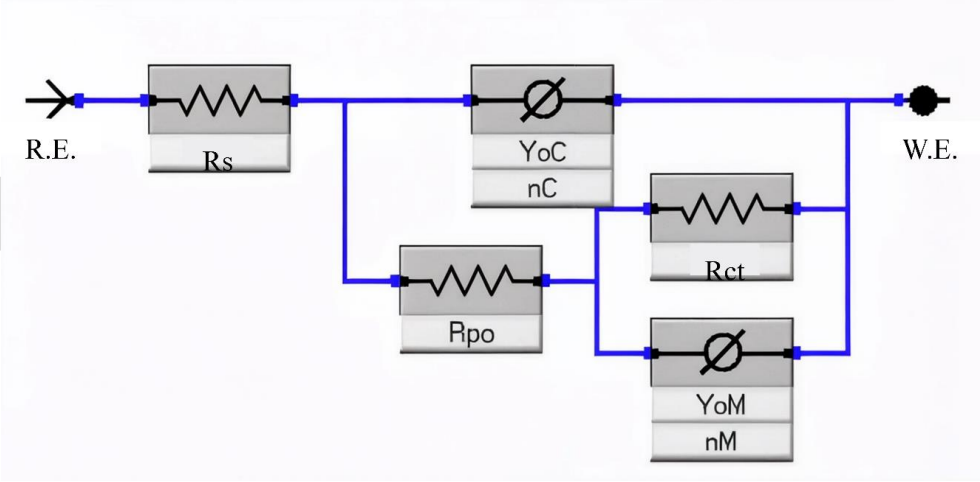

Figure 1: EEC used for FBE and hybrid epoxy coatings

The impedance plots for the FBE coating displayed ideal capacitive behavior throughout the 21-day immersion period. As seen in the Bode plots (Figure 2) for FBE samples in the Persian Gulf environment, the low-frequency impedance modulus ($|Z|_{10mHz}$) remained

very high and showed no significant change over time. Additionally, the coating capacitance (C_c) and pore resistance (R_{po}) values, presented in Figure 3a and Figure 3b, remained approximately constant. The stability of these parameters indicates that the FBE coating exhibited no detectable degradation within the 21-day immersion period under the tested environments and temperatures [30]. Nevertheless, longer-term immersion/testing is required to confirm whether this behavior persists over extended service durations beyond the timeframe investigated in this study.

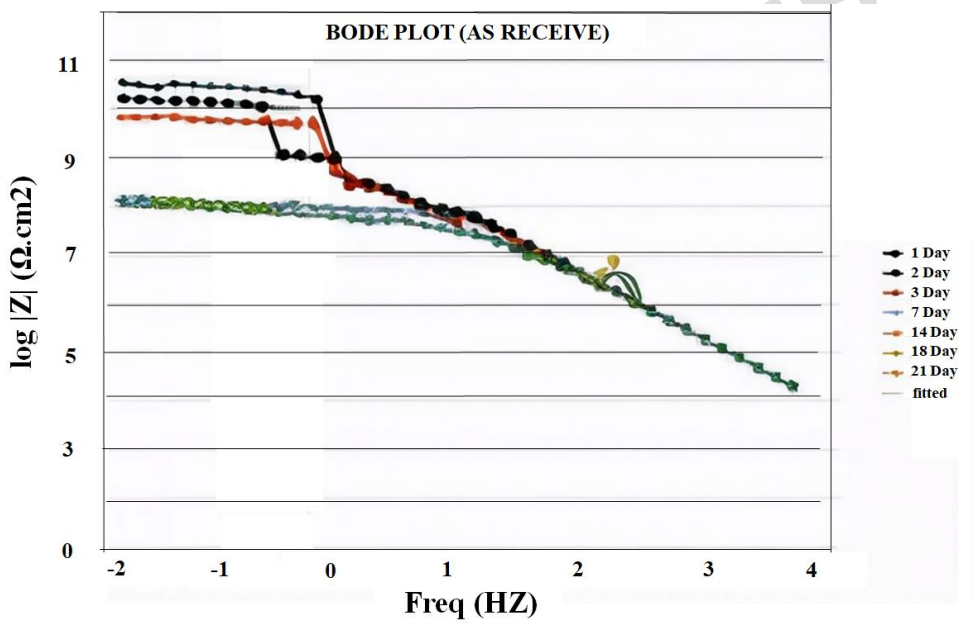

Figure 2: Bode plot for PBE coverage in the Persian Gulf at 36°C

However, unlike FBE, the Hybrid Epoxy coating showed clear signs of degradation, particularly in the Persian Gulf environment. Results indicated that the coating capacitance (C_c) increased over time, signifying water uptake and a reduction in dielectric properties. Furthermore, the pore resistance (R_{po}) for Hybrid Epoxy was initially lower in the Persian Gulf environment and declined sharply over time. The significant drop in the low-frequency impedance modulus ($|Z|_{10mHz}$), evident in Figure 3c, provides further

indicates the reduced resistance of the coating system and its degradation over time. The reliability of the EIS fitting was assessed using the χ^2 goodness-of-fit parameter, with all fitted spectra exhibiting low χ^2 values on the order of 10^{-4}-10^{-3}, confirming excellent agreement between the experimental impedance data and the corresponding equivalent electrical circuit models.

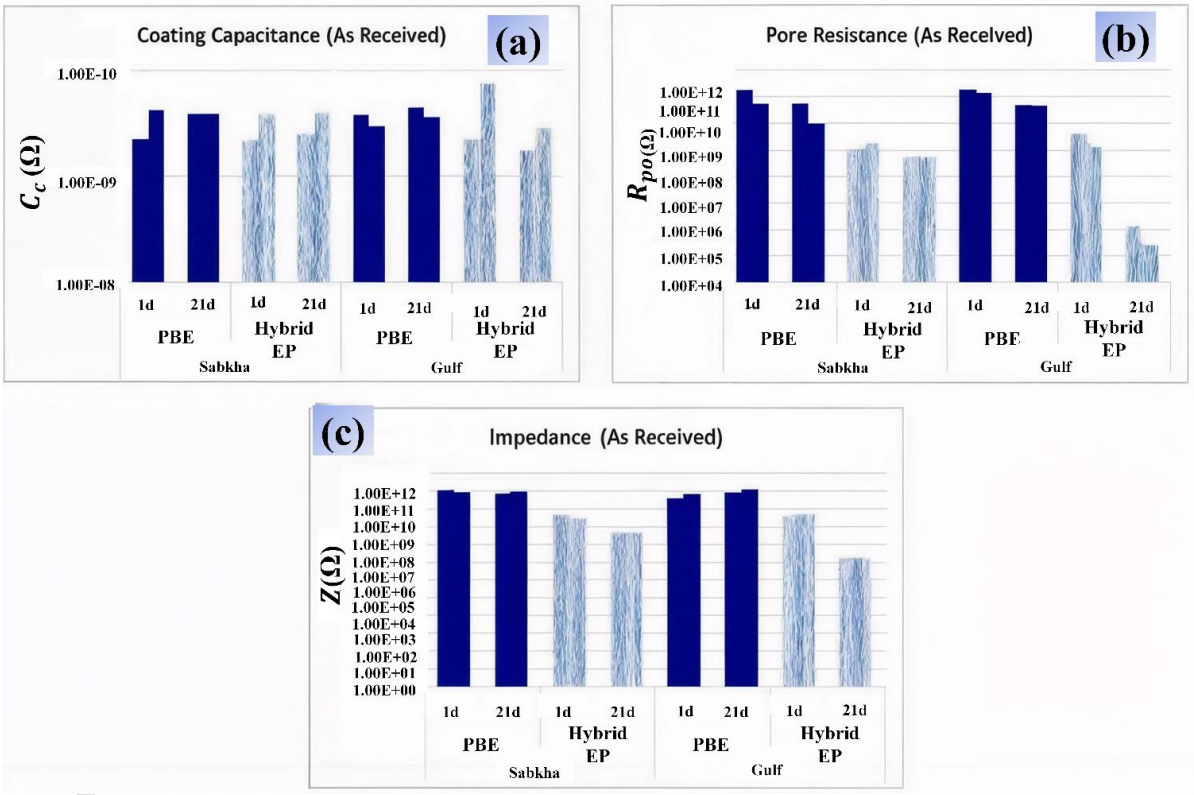

Figure 3: (a) the coating capacitance (C_c), (b) the pore resistance (R_{po}), and impedance values for the FBE and Hybrid Epoxy coatings in the Persian Gulf and Sabkha environments. The reported C_c, and R_{po} represent averaged values from replicate measurements, with standard deviations in the range of 3-8%.

3.2. Corrosion behavior under defect and cathodic disbondment

To assess the performance of the coating in a practical damage condition, electrochemical studies were performed on the scratched specimens and the specimens undergoing cathodic disbondment (CD) tests in the Sabkha environment and the Persian Gulf environment. Linear Polarization Resistance (LPR) studies carried out on the scratched

specimens show that the FBE and Hybrid Epoxy coats recorded a substantial corrosion current in the period of 21 days, along with the formation of corrosion products in the damaged area (Figure 4). Comparative studies across the two environments suggest that corrosion current values in the Persian Gulf are higher than those in the Sabkha, due to the higher dissolved oxygen concentration in Persian Gulf water, which significantly accelerates cathodic reactions in the test environment. Comparing the quantitative results of the LPR studies of the scratched specimens, the Hybrid Epoxy coating performed relatively better than the FBE coating. Based on the results, the corrosion current intensity of the Hybrid Epoxy coating was lower than the FBE coating in both environments.

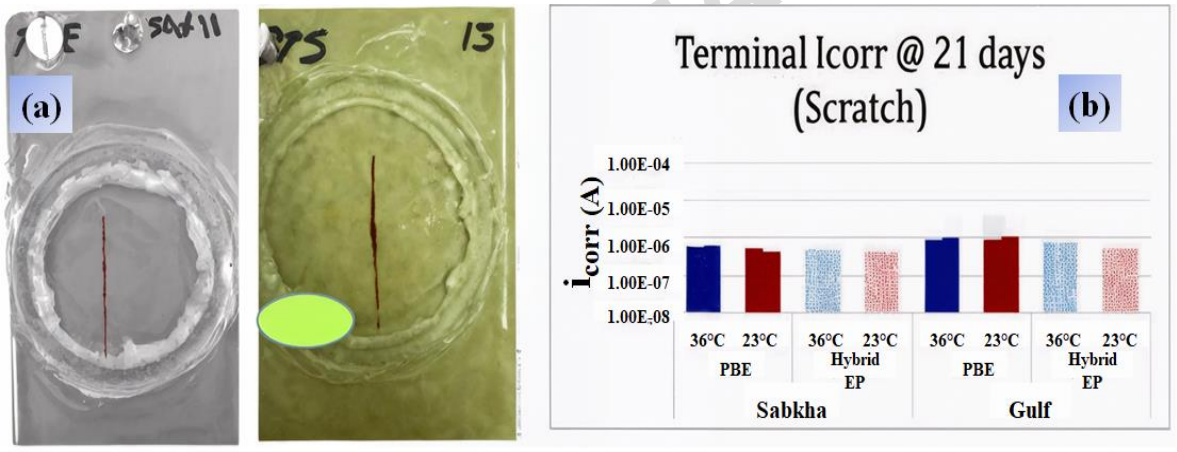

Figure 4: (a) Digital images of scratched PBE and hybrid epoxy coatings in Sabkha and Persian Gulf environments and (b) i_{corr} value for scratched PBE and hybrid epoxy coatings in Sabkha and Persian Gulf environments. The reported i_{corr} represent averaged values from replicate measurements, with standard deviations in the range of 3-8%.

Moreover, based on the results of EIS studies of the scratched specimens (Figure 5a and 5b), a comparison of the $|Z|_{10mHz}$ has confirmed that the values for the specimens immersed in the Persian Gulf are lower than those in the Sabkha environment, proving the higher severity of the Persian Gulf environment. Moreover, the increase in the values of the Constant Phase Element (CPE) over time in both specimens (Figure 5c) indicates

growth of the electrolyte and active corrosion areas behind the coating due to electrolyte infiltration through the coating and the increase in the active corrosion area at the defect [31, 32].

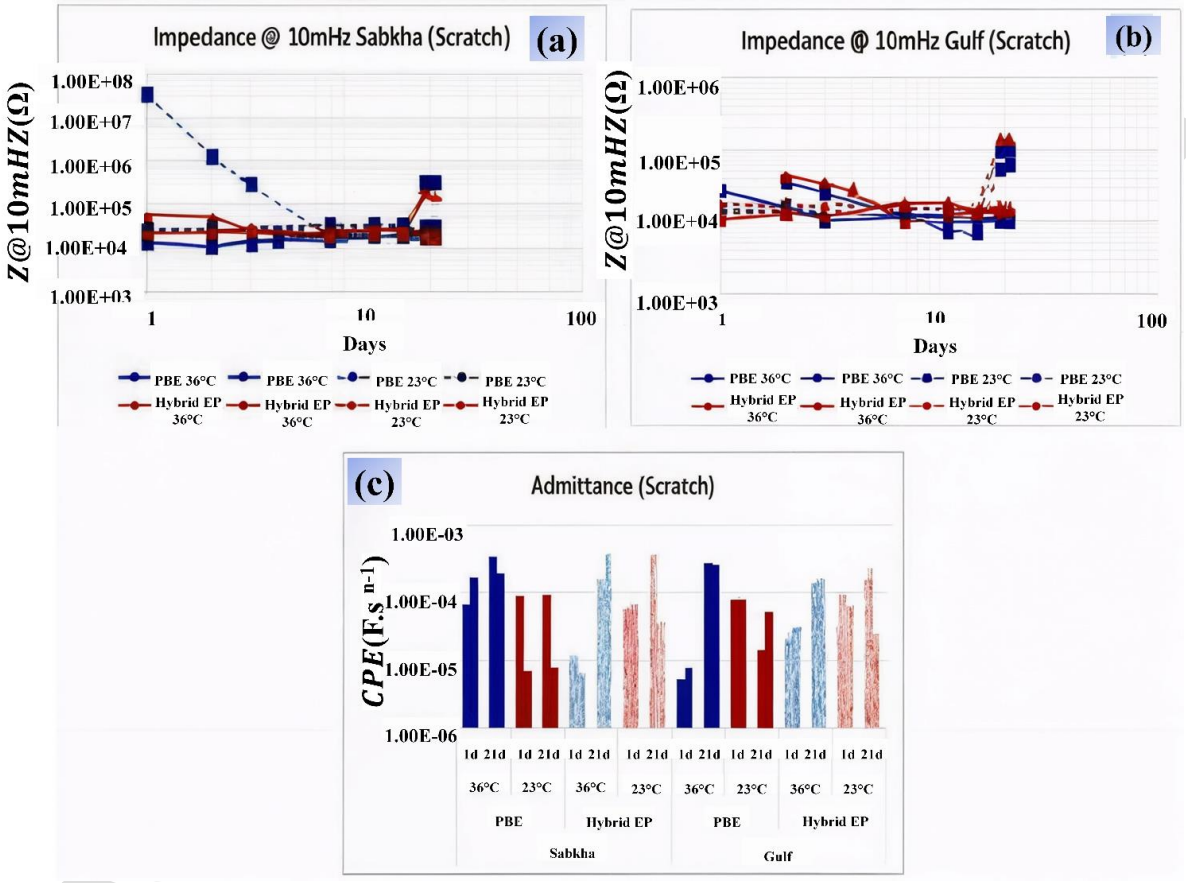

Figure 5: (a) Impedance trend for scratched PBE and hybrid epoxy coatings in Sabkha, (b) Impedance trend for PBE and hybrid epoxy coatings in Persian Gulf, and (c) CPE results for scratched PBE and hybrid epoxy coatings. The reported CPE represent averaged values from replicate measurements, with standard deviations in the range of 3–8%.

For the cathodic disbondment (CD) tests, which are a severe environment for buried pipelines when applying cathodic protection, coating growth of corrosion products was observed on both coating samples after exposure to negative potential for 21 days (Figure 6a). The LPR test results for the samples (Figure 6b) suggest that the cumulative value of the i_{corr} is higher in the Persian Gulf environment and tends to increase with an increase in

temperature. The comparison of the two coating samples in the cathodic disbondment test environment shows that the Hybrid Epoxy coating has a lower value of cumulative i_{corr} at higher temperatures (36 °C) than FBE, while in the lower temperature environment (23 °C), FBE has higher values.

Additional analyses employing the EIS technique for the cathodic disbondment specimens (Figures 6c and 6d) supported the results of the LPR studies. The impedance values recorded for the Hybrid Epoxy in the cathodic disbondment environment were higher than those recorded for the FBE coating specimens. The results imply that the Hybrid Epoxy coating has better cathodic disbondment corrosion resistance and more stable performance than the FBE coating in a highly oxygenated environment, characteristic of the Persian Gulf. The temperature effect was particularly pronounced for the FBE coating under cathodic disbondment conditions. At 36 °C in Persian Gulf seawater, the FBE system exhibited a ~100% increase (approximately doubled) in cumulative corrosion current density compared to 23 °C, whereas the Hybrid coating showed only a ~10% increase under identical conditions. This temperature sensitivity can be attributed to accelerated water diffusion through the FBE microstructure and reduced interfacial bond stability at elevated temperatures, consistent with thermal activation of degradation mechanisms [8, 33].

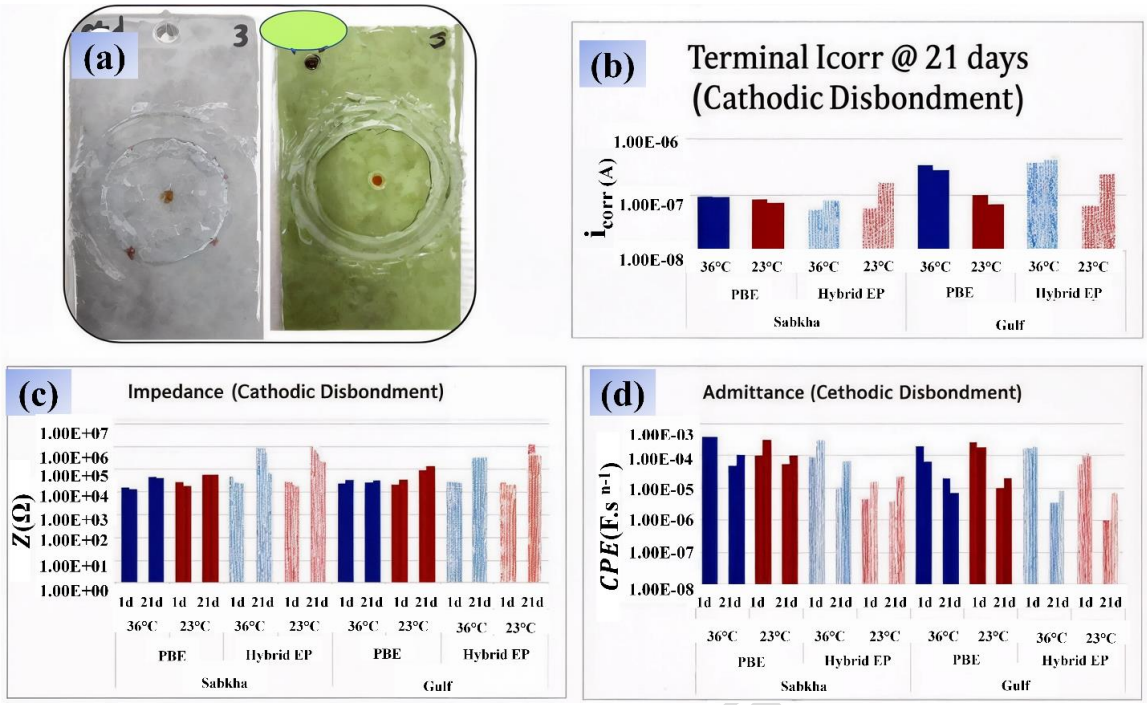

Figure 6: (a) Digital images of PBE and hybrid epoxy coatings, (b) i_{corr} values, (c) Impedance values, and (d) CPE results for cathodic disbondment coated panels in Sabkha and Persian Gulf environments at temperatures of 23 and 36°C. The reported i_{corr}, and CPE represent averaged values from replicate measurements, with standard deviations in the range of 3-8%.

3.3. Evaluation of mechanical properties and adhesion stability

The stability of the coating/metal interface and resistance to disbonding forces are critical parameters for predicting the service life of buried pipelines. In this study, the adhesion strength was quantitatively assessed using the Pull-off Adhesion Test (according to ASTM D-4541), and qualitatively evaluated using the Knife Test (in accordance with NACE RP-0394).

3.3.1. Adhesion strength under initial and mechanically damaged conditions

The results of the Pull-off test for as-received samples, presented in Figure 7a-c, demonstrated ideal adhesive behavior. As shown in Figure 7a, the failure mode observed for all specimens was "glue failure". The occurrence of this failure mode indicates that

the bond strength between the polymeric coating and the steel substrate exceeded the tensile strength of the epoxy adhesive used to bond the dolly to the coating surface. The measured adhesion strength values, shown in the charts of Figure 7b, consistently exceeded 1000 psi, confirming the excellent initial adhesion of both the FBE and Hybrid Epoxy systems. This high level of adhesion stability was maintained even in the presence of intentional mechanical defects. As shown in Figure 7c, even for the scratched specimens in both Sabkha and Gulf seawater environments, failure remained cohesive within the glue, and no reduction in adhesion strength was observed in the regions adjacent to the scribe, attesting to the high integrity of the coatings.

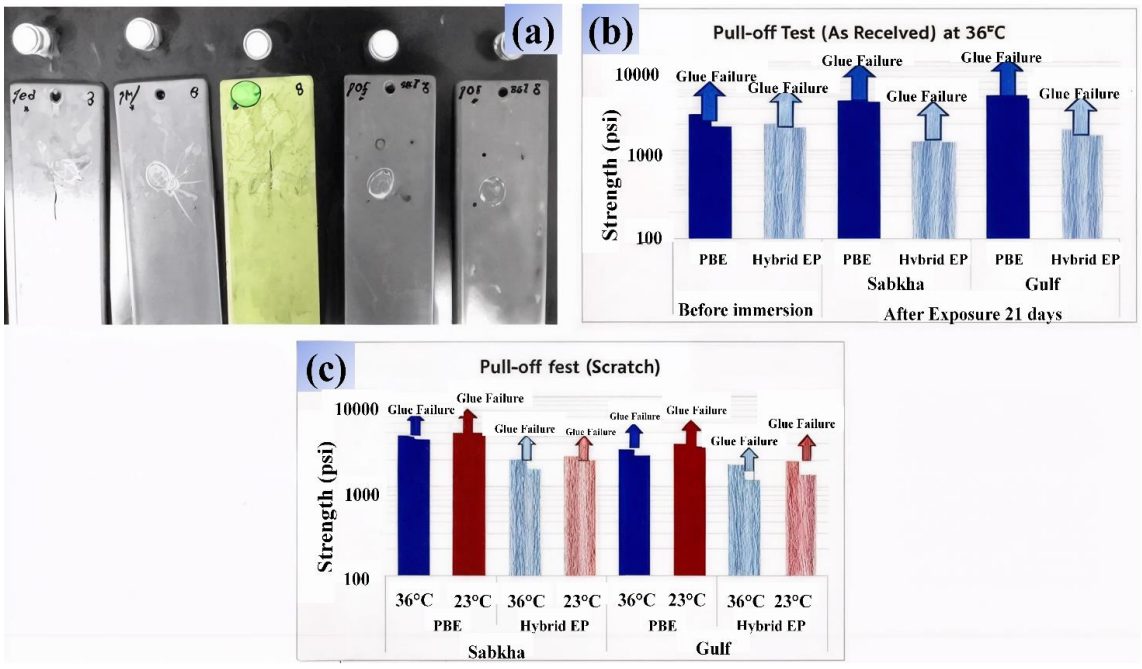

Figure 7: (a) Digital images of samples after Pull-off, (b) Pull-off adhesion results for the as received coated plates, (c) Pull-off adhesion results for the scratched coated plates.

3.3.2. Adhesion evaluation under CD conditions

The adhesive behavior of the coatings underwent noticeable changes after application of a cathodic protection potential and exposure to a corrosive environment for 21 days. As

illustrated in Figure 8a, due to the limited surface area of the disbonded region relative to the test dolly diameter in the affected areas of CD, performing the standard Pull-off Test to measure the exact disbonding force was not feasible. Therefore, the Knife Test was employed to assess the interface resistance to peeling, as depicted in Figure 8b. Analysis of the Knife Test results, summarized in Figure 8c, revealed that the Hybrid Epoxy coating exhibited a distinct performance with a rating of 2 (according to the NACE standard) in the Gulf seawater environment. This indicates the coating's high resistance to the alkaline forces generated by cathodic reactions. Conversely, the FBE coating in Gulf seawater demonstrated dramatically greater sensitivity to environmental conditions at the elevated temperature of 36°C. The disbondment occurred with significantly greater ease at 36°C compared to 23°C, and this temperature-accelerated degradation was more severe in the Gulf environment than in Sabkha conditions, highlighting the synergistic effect of high temperature, high dissolved oxygen, and cathodic polarization on FBE interfacial stability.

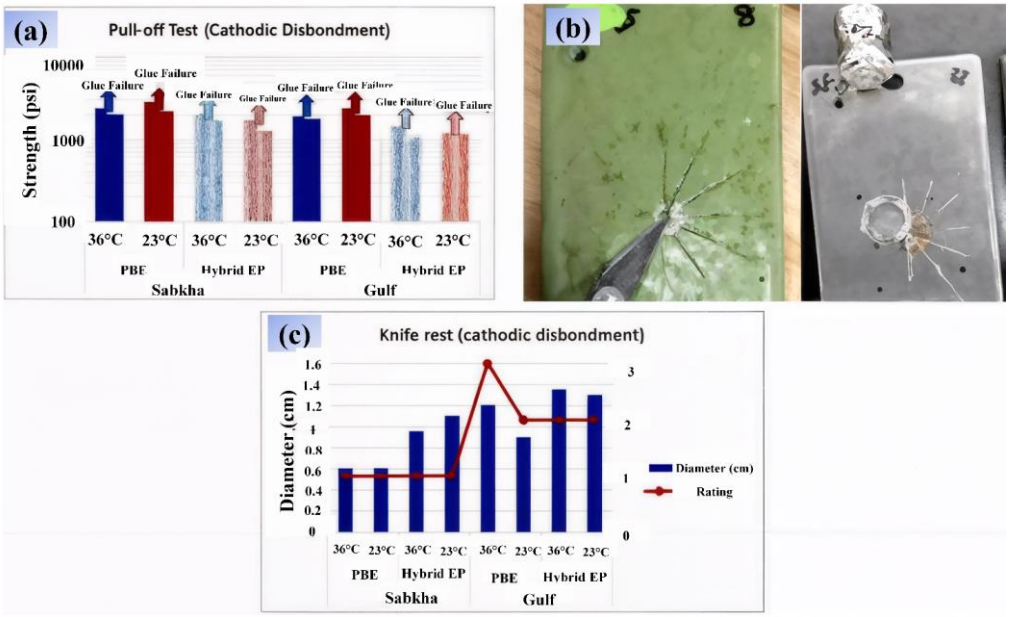

Figure 8: (a) Pull-off adhesion results for cathodic disbondment coated panels, (b) Digital image of knife test and pull-off test, (c) Knife test results for cathodic disbondment coated panels.

3.3.3. Substrate observations post-disbondment

A close inspection of the substrate surface in Figure 8b, which illustrates the effect of the Knife Test, clearly shows a fundamental disparity in the process of substrate degradation between the two coating materials. The disbondment of the steel substrate from the FBE coating led to the formation of corrosion products in the disbonded zone. The presence of corrosion products in the disbonded area indicates that the diffusion of aggressive species and oxygen in the environment was facilitated by the FBE coating, thereby resulting in considerable substrate corrosion beneath the coating film. It is clear that the substrate surface underneath the Hybrid Epoxy coating remains clean and free from corrosion products resulting from the disbondment process.

3.4. Morphological characterization and failure mechanisms

To verify the measured electrochemical properties and provide a clear understanding of the coating degradation mechanisms, Optical Microscopy (OM) and SEM were used. The first microscopic investigation of the intact specimens demonstrated that the samples treated with FBE and Hybrid Epoxy coats have a relatively smooth surface, but blisters of various diameters are observed due to metallic fillers in the polymer matrix. A more detailed investigation of the structure of the two coating samples in the "intact" state, shown in Figure 9, reveals a more porous, larger-pore-diameter structure in the Hybrid Epoxy coating than in the FBE coating. The noted structural differences and the presence of large pores in the Hybrid Epoxy coating confirm a decrease in its pore resistance over time, as described by the relationship for electrolyte resistance in pores. Based on the observations, the structural properties confirm that the two samples exhibit relatively

excellent performance and that the denser structure of the FBE coating results in higher impedance and greater corrosion resistance in the intact state.

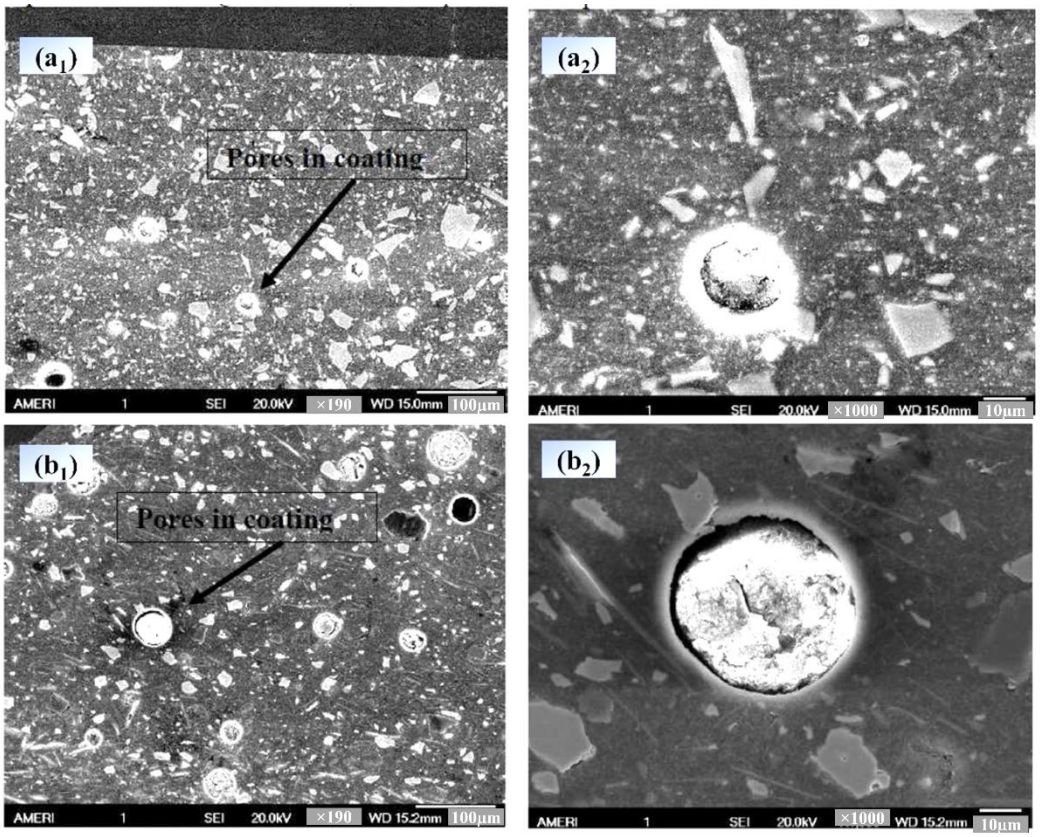

Figure 9: SEM examination of (a_1-a_2) PBE coating at 190x and 1000x magnifications, and (b_1-b_2) Hybrid Epoxy coating at 190x and 1000x magnifications

For samples with surface defects (scratches), SEM images confirmed the large difference in corrosion rates between the Persian Gulf and Sabkha environments. For the Persian Gulf environment, the SEM images of the FBE coating and the Hybrid Epoxy coating (Figure 10) confirmed the presence of corrosion creep of approximately 152 µm on one side and a more severe corrosion creep of approximately 177 µm on both sides of the scratch, respectively, attaining the penetration of the corrosive solution to the interface of the coating and substrate.

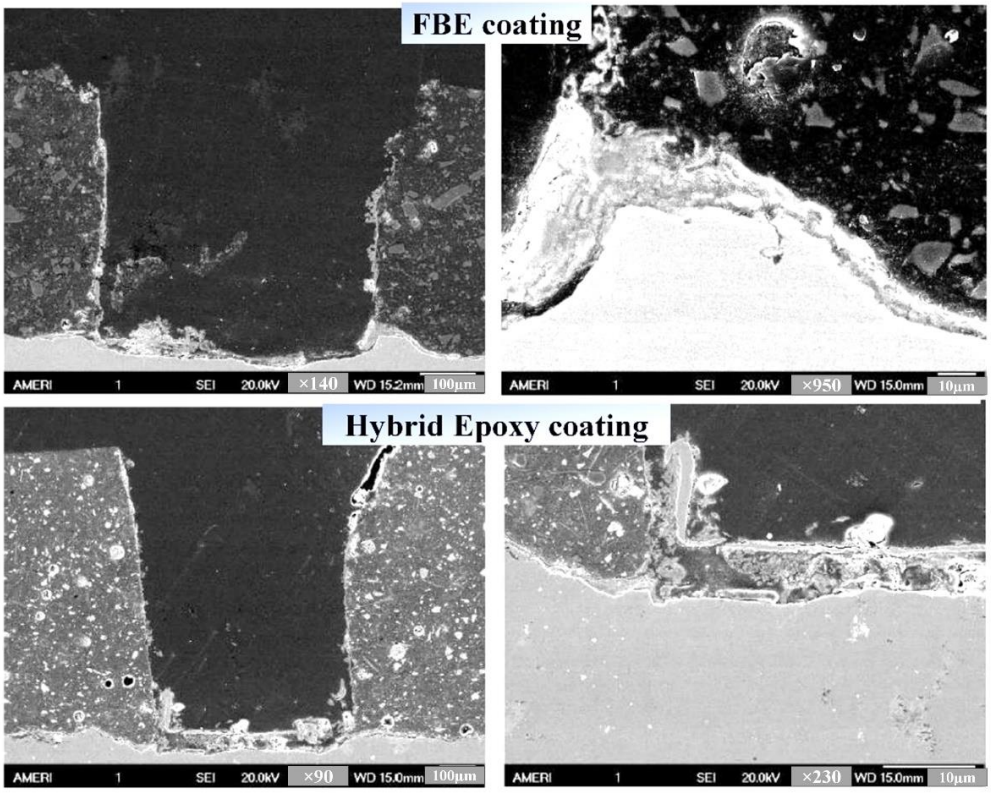

Figure 10: FE-SEM images of scratched PBE and Hybrid Epoxy coatings in the Persian Gulf environment

For the samples in the Sabkha environment, the investigation of the corresponding images for the FBE coating and the Hybrid Epoxy coating (Figure 11) confirmed that there was no corrosion creep and delamination at the interface but the corrosion was restricted to the growth of products in the scratched areas only, an observation that is in excellent accord with the results reported in the electrochemical measurements and confirming the more aggressive and higher corrosion currents in the Persian Gulf environment than in the Sabkha environment by a large margin.

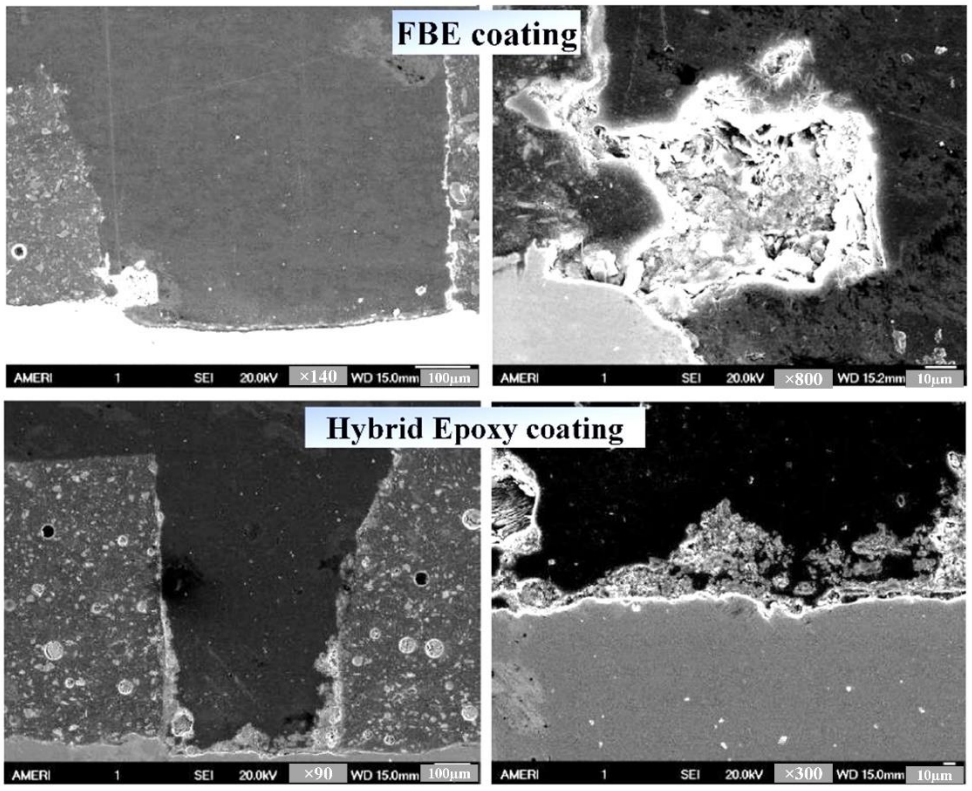

Figure 11: FE-SEM images of scratched PBE and Hybrid Epoxy coatings in the Sabkha environment.

The results of the failure mechanism analysis of specimens undergoing cathodic disbondment (CD) tests also highlighted the presence of crevice corrosion and the effect of crevice geometry on coating performance. Based on the theory of crevice corrosion, reduced convection in the disbonded area promotes an oxygen-depleted environment and the diffusion of chlorides into the crevice, making the environment highly corrosive and acidic [34,35]. Optical Microscopy (OM) of the Hybrid Epoxy and substrate interface (Figure 12) demonstrated the tendency of the coating to disbond via an "Oxide Lift" process, in which anodic corrosion products accumulate and lift the coating off the substrate entirely. The presence of a wider crevice in the Hybrid Epoxy allowed the heavier corrosion products to accumulate. In the FBE coating images (Figure 13), many areas showed pitting corrosion at the interface. The results indicate the presence of a

"Tight Crevice" in FBE, leading to aggressive chemical concentrations and a severe corrosion environment behind the coating. The fact that FBE easily peels off because of the "oxide lift effect" and the presence of a higher area associated with convection in the crevice than other specimens, such as the Hybrid Epoxy samples, reveals the process of cathodic disbondment in FBE.

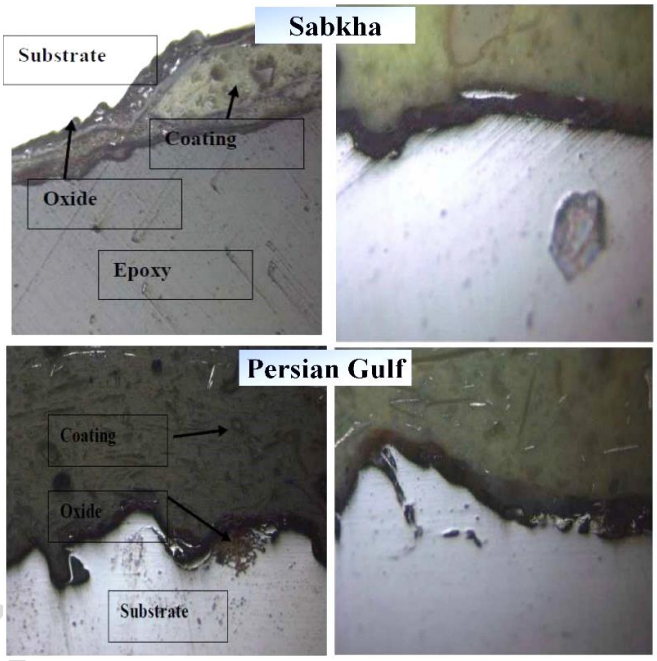

Figure 12: Optical Microscopy for epoxy hybrid interface in Sabkha and Persian Gulf environment.

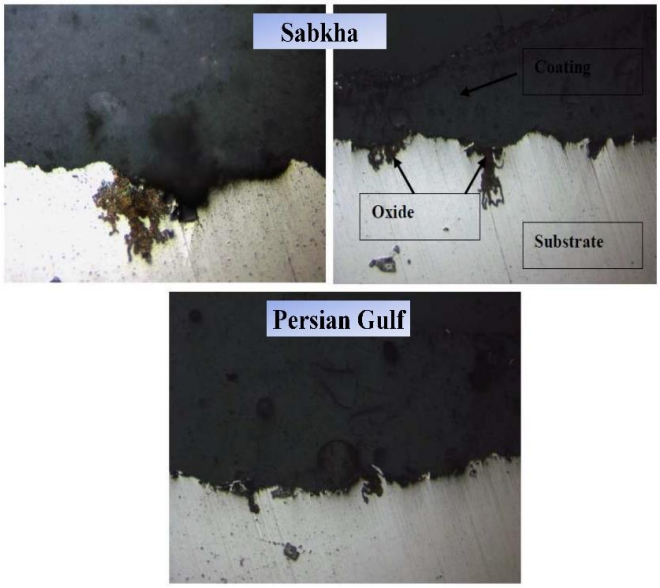

Figure 13: Optical Microscopy for FBE interface in Sabkha and Persian Gulf environment.

4. Conclusion

This study evaluated the performance of Fusion-Bonded Epoxy (FBE) and a Hybrid Epoxy coating system under conditions simulating Sabkha soil and Persian Gulf seawater at temperatures of 23°C and 36°C. The results reveal a critical distinction between the primary barrier performance and damage tolerance of the two systems. In intact conditions, the FBE coating demonstrated superior primary isolation, characterized by consistently higher impedance values and lower capacitance compared to the hybrid system across the tested environments. Conversely, the Hybrid Epoxy exhibited significantly higher damage tolerance when subjected to mechanical defects and cathodic protection. Under cathodic disbondment conditions, the Hybrid coating effectively resisted the alkaline environment at the cathode, maintaining a NACE rating of 2 in Persian Gulf seawater, whereas the FBE coating showed greater susceptibility to disbondment, particularly at 36°C.

A critical finding is the strong temperature dependence of FBE performance, with the

36°C condition resulting in substantially higher cathodic disbondment susceptibility and corrosion rates compared to 23°C, while the Hybrid system demonstrated better thermal stability across the tested temperature range.

Quantitative mechanical testing confirmed that both coating systems possess excellent initial adhesion. Pull-off adhesion tests for both FBE and Hybrid Epoxy consistently yielded values exceeding 1000 psi in the "glue failure" mode, indicating that the coating-substrate bond strength exceeded the adhesive's cohesive strength, even in the presence of surface scratches. However, long-term stability varied, with the FBE showing greater sensitivity to oxide lift and delamination in the warm, saline Gulf environment than in the Sabkha conditions. It is important to note that these findings are specific to the high-salinity, sulfate-rich chemistries of the Sabkha and Persian Gulf environments within the 23°C to 36°C temperature range. Consequently, the superior damage tolerance of the Hybrid system or the barrier dominance of the FBE observed here should not be extrapolated to environments with significantly different ionic compositions or operating temperatures without further experimental validation. These findings are limited to the two simulated electrolytes, 23–36°C, and a 21-day exposure period; longer-term exposures and complementary accelerated atmospheric tests (e.g., salt spray) are recommended as future work.

References

1. Chen C, Li C, Reniers G, Yang F. Safety and security of oil and gas pipeline transportation: A systematic analysis of research trends and future needs using WoS. J Clean Prod. 2021; 279: 123583. https://doi.org/10.1016/j.jclepro.2020.123583

2. Montemor MF, Vicente C. Functional self-healing coatings: a new trend in corrosion protection by organic coatings. Encyclopedia Interf Chem: Surf Sci Electrochem. 2018; 236-249. https://doi.org/10.1016/B978-0-12-409547-2.13442-0

3. Kardar P. Preparation of polyurethane microcapsules with different polyols component for encapsulation of isophorone diisocyanate healing agent. Prog Org Coat. 2015; 89: 271-276. https://doi.org/10.1016/j.porgcoat.2015.09.009

4. Bonvicini S, Antonioni G, Cozzani V. Assessment of the risk related to environmental damage following major accidents in onshore pipelines. J Loss Prev Process Ind. 2018; 56: 505-516. https://doi.org/10.1016/j.jlp.2018.11.005

5. Prasad AR, Kunyankandy A, Joseph A. Corrosion inhibition in oil and gas industry: economic considerations. Corr Inhibitor Oil Gas Indust. 2020; 135-150. https://doi.org/10.1002/9783527822140.ch5

6. Hakami A, Ghrefat H, Elwaheidi M, Galmed M, Yahya MA. Assessment of the corrosivity of the Southern Red Sea coastal sabkha soil: an integrated mineralogical, geochemical, and GIS approach. Environ Earth Sci. 2022; 81: 225. https://doi.org/10.1007/s12665-022-10316-w

7. Zhang Z, Yan D, Liu X, Li W, Wang Z, Wang Y, et al. Self-healing nanocomposite coatings containing organic-inorganic inhibitors functionalized dendritic silica nanocontainers for synergistic corrosion protection of carbon steel. Colloids Surf A Physicochem Eng Asp. 2022; 130430. https://doi.org/10.1016/j.colsurfa.2022.130430

8. Davarpanah A, Haddadi SA, Ramezanzadeh M, Ramezanzadeh B, Mekonnen TH. Covalent organic framework (COF)-enhanced carbon hollow sphere (CS): a novel

nano-porous material for robust epoxy composite coating intelligent corrosion protection. Adv Composite Hybrid Mater. 2025; 8: 334. https://doi.org/10.1007/s42114-025-01408-9

9. Honarvar Nazari M, Zhang Y, Mahmoodi A, Xu G, Yu J, Wu J, et al. Nanocomposite organic coatings for corrosion protection of metals: A review of recent advances. Prog Org Coat. 2022; 162: 106573. https://doi.org/10.1016/j.porgcoat.2021.106573

10. Kardar P, Ebrahimi M, Bastani S. Influence of temperature and light intensity on the photocuring process and kinetics parameters of a pigmented UV curable system. J Thermal Anal Calorimetry. 2014; 118(1): 541-549. https://doi.org/10.1007/s10973-014-3984-z

11. Ramezanzadeh B, Rostami M. The effect of cerium-based conversion treatment on the cathodic delamination and corrosion protection performance of carbon steel-fusion-bonded epoxy coating systems. Appl Surf Sci. 2017; 392: 1004-1016. https://doi.org/10.1016/j.apsusc.2016.09.140

12. Baig MMA, Samad MA. Epoxy/epoxy composite/epoxy hybrid composite coatings for tribological applications—a review. Polymers. 2021; 13: 179. https://doi.org/10.3390/polym13020179

13. Białkowska A, Bakar M, Kucharczyk W, Zarzyka I. Hybrid epoxy nanocomposites: improvement in mechanical properties and toughening mechanisms—a review. Polymers. 2023; 15: 1398. https://doi.org/10.3390/polym15061398

14. Sadowski Ł, Kampa Ł, Chowaniec A, Królicka A, Żak A, Abdoulpour H, et al. Enhanced adhesive performance of epoxy resin coating by a novel bonding agent.

Constr Build Mater. 2021; 301: 124078. https://doi.org/10.1016/j.conbuildmat.2021.124078

15. Hossain S, Islam MS, Islam MA, Hasib MA, Shaikh MS. Effect of silicon carbide on enhancing interfacial adhesion and mechanical properties of Kevlar-glass fiber hybrid composites. Hybrid Adv. 2025; 11: 100534. https://doi.org/10.1016/j.hybadv.2025.100534

16. Mahdavi F, Forsyth M, Tan MYJ. Understanding the effects of applied cathodic protection potential and environmental conditions on the rate of cathodic disbondment of coatings by means of local electrochemical measurements on a multi-electrode array. Prog Org Coat. 2017; 103: 83-92. https://doi.org/10.1016/j.porgcoat.2016.10.020

17. Mahdavi F, Forsyth M, Tan MYJ. Techniques for testing and monitoring the cathodic disbondment of organic coatings: An overview of major obstacles and innovations. Prog Org Coat. 2017; 105: 163-175. https://doi.org/10.1016/j.porgcoat.2016.11.034

18. Cao Q, Oluwoye I, Pojtanabuntoeng T, Farhat H, Iannuzzi M. Evaluation of epoxy-based coating degradation under thermal insulation at elevated temperatures on different steel substrates. Prog Org Coat. 2023; 180: 107544. https://doi.org/10.1016/j.porgcoat.2023.107544

19. Ramezanzadeh B, Kardar P, Bahlakeh G, Hayatgheib Y, Mahdavian M. Fabrication of a highly tunable graphene oxide composite through layer-by-layer assembly of highly crystalline polyaniline nanofibers and green corrosion inhibitors: complementary experimental and first-principles quantum-mechanics modeling

approaches. J Phys Chem C. 2017; 121: 20433-20450. https://doi.org/10.1021/acs.jpcc.7b04323

20. Davarpanah A, Bahlakeh G, Ramezanzadeh B. Engineering a novel smart nano-carrier based on NH2-MIL-125 metal-organic framework (Ti-MOF) decorated 2D GO nano-platform for reaching a self-healing coating. Appl Mater Today. 2023; 32: 101844. https://doi.org/10.1016/j.apmt.2023.101844

21. Gateman SM, Gharbi O, Gomes de Melo H, Ngo K, Turmine M, Vivier V. On the use of a constant phase element (CPE) in electrochemistry. Curr Opin Electrochem. 2022; 36: 101133. https://doi.org/10.1016/j.coelec.2022.101133

22. Alexander CL, Tribollet B, Orazem ME. Contribution of surface distributions to constant-phase-element (CPE) behavior: 1. influence of roughness. Electrochim Acta. 2015; 173: 416-424. https://doi.org/10.1016/j.electacta.2015.05.010

23. Kim YJ, Bahn CB, Baek SH, Choi W, Song GD. Crevice chemistry and corrosion in high temperature water: A review. Nuclear Eng Technol. 2024; 56: 3112-3122. https://doi.org/10.1016/j.net.2024.03.010

24. Haddadi SA, Ghaderi S, Sadeghi M, Gorji B, Ahmadijokani F, Ramazani SAA, et al. Enhanced active/barrier corrosion protective properties of epoxy coatings containing eco-friendly green inorganic/organic hybrid pigments based on zinc cations/Ferula Asafoetida leaves. J Mol Liq. 2021; 323: 114584. https://doi.org/10.1016/j.molliq.2020.114584

25. Zhao Z, Zhou M, Zhao W, Hu J, Fu H. Anti-corrosion epoxy/modified graphene oxide/glass fiber composite coating with dual physical barrier network. Prog Org Coat. 2022; 167: 106823. https://doi.org/10.1016/j.porgcoat.2022.106823

26. Ramezanzadeh B, Bahlakeh G, Mohamadzadeh Moghadam MH, Miraftab R. Impact of size-controlled p-phenylenediamine (PPDA)-functionalized graphene oxide nanosheets on the GO-PPDA/Epoxy anti-corrosion, interfacial interactions and mechanical properties enhancement: Experimental and quantum mechanics investigations. Chem Eng J. 2018; 335: 737-755. https://doi.org/10.1016/j.cej.2017.11.019

27. Kester DR, Duedall IW, Connors DN, Pytkowicz RM. Preparation of artificial seawater. Limnol Oceanography. 1967; 12: 176-179. https://doi.org/10.4319/lo.1967.12.1.0176

28. Grimme S. Semiempirical GGA-type density functional constructed with a long-range dispersion correction. J Comput Chem. 2006; 27: 1787-1799. https://doi.org/10.1002/jcc.20495

29. Saleh TA, Satria M, Nur MM, Aljeaban N, Alharbi B. Synthesis of vinyl trimethyl silane and acrylic acid modified silica nanoparticles as corrosion inhibition protocols in saline medium. Fuel. 2023; 339: 127277. https://doi.org/10.1016/j.fuel.2022.127277

30. Chang W, Wang P, Zhao Y, Ren C, Popov BN, Li C. Characterizing corrosion properties of graphene barrier layers deposited on polycrystalline metals. Surf Coat Technol. 2020; 398: 126077. https://doi.org/10.1016/j.surfcoat.2020.126077

31. Davarpanah A, Keramatinia M, Soroush E, Nouri N, Ramezanzadeh B. Improving the polyester powder coating self-healing anti-corrosion properties via the steel surface decoration with Ce-doped-ZIF-8@ZPMn film. Surf Interfac. 2023; 41: 103144. https://doi.org/10.1016/j.surfin.2023.103144

32. Yan D, Wang Y, Liu J, Song D, Zhang T, Liu J, et al. Self-healing system adapted to different pH environments for active corrosion protection of magnesium alloy. J Alloys Compd. 2020; 824: 153918. https://doi.org/10.1016/j.jallcom.2020.153918

33. Alibakhshi E, Ghasemi E, Mahdavian M, Ramezanzadeh B. A comparative study on corrosion inhibitive effect of nitrate and phosphate intercalated Zn-Al-layered double hydroxides (LDHs) nanocontainers incorporated into a hybrid silane layer and their effect on cathodic delamination of epoxy topcoat. Corros Sci. 2017; 115: 159-174. https://doi.org/10.1016/j.corsci.2016.12.001

34. Soroush E, Davarpanah A, Keramatinia M, Nouri N, Ramezanzadeh B. Synergistic impact of the functionalized graphene oxide (fGO) nano-sheets and Mn2+-doped zinc phosphate conversion film on the polyester coating corrosion protection properties. Colloids Surf A Physicochem Eng Asp. 2023; 678: 132510. https://doi.org/10.1016/j.colsurfa.2023.132510

35. Vautrin-Ul C, Mendy H, Taleb A, Chausse A, Stafiej J, Badiali JP. Numerical simulations of spatial heterogeneity formation in metal corrosion. Corros Sci. 2008; 50: 2149-2158. https://doi.org/10.1016/j.corsci.2008.03.012